Journal of Power Sources 196 (2011) 7681–7686

Contents lists available at ScienceDirect

Journal of Power Sources

journal homepage: www.elsevier.com/locate/jpowsour

Effect of co-doping nano-silica filler and *N*-methyl-*N*-propylpiperidinium bis(trifluoromethanesulfonyl)imide into polymer electrolyte on Li dendrite formation in Li/poly(ethylene oxide)-Li$(CF_3SO_2)_2N$/Li

S. Liu [a,b], H. Wang [b], N. Imanishi [b,*], T. Zhang [b], A. Hirano [b], Y. Takeda [b], O. Yamamoto [b], J. Yang [a]

[a] School of Material Science and Engineering, Shanghai Jiao Tong University, Shanghai 200020, PR China
[b] Department of Chemistry, Faculty of Engineering, Mie University, 1577 Kurimamachiyacho, Tsu, Mie 514-8507, Japan

ARTICLE INFO

Article history:
Received 14 January 2011
Received in revised form 1 April 2011
Accepted 1 April 2011
Available online 20 April 2011

Keywords:
Dendrite
Ionic liquid
Ceramic filler
Lithium metal
Lithium air battery

ABSTRACT

Lithium metal dendrite growth in Li/poly (ethylene oxide)-lithium bis (trifluoromethanesulfonyl) imide (PEO_{18}LiTFSI), nano-silica, and *N*-methyl-*N*-propylpiperidinium bis(trifluoromethanesulfonyl)imide (PP13TFSI) composite solid polymer electrolyte/Li was investigated by direct *in situ* observation. The dendrite onset time decreased with increasing current density and deviated from Sand's law in the current density range of 0.1–0.5 mA cm^{-2} at 60 °C. Lithium dendrite formation was not observed until 46 h of polarization at 0.5 mA cm^{-2} and 60 °C, which is a significant improvement compared to that observed in Li/(PEO_{18}LiTFSI)/Li, where the dendrite formation was observed after 15 h polarization at 0.5 mA cm^{-2} and 60 °C. The suppression of dendrite formation could be explained by the electrical conductivity enhancement and decrease of the interface resistance between Li and the polymer electrolyte by the introduction of both nano-SiO_2 and PP13TFSI into PEO_{18}LiTFSI. The electrical conductivity of 4.96×10^{-4} S cm^{-1} at 60 °C was enhanced to 7.6×10^{-4} S cm^{-1}, and the interface resistance of Li/PEO_{18}LiTFSI/Li of 248 Ω cm^2 was decreased to 74 Ω cm^2 by the addition of both nano-SiO_2 and PP13TFSI into PEO_{18}LiTFSI.

1. Introduction

The motivation for using lithium metal as an anode for high energy density batteries lies in its high theoretical specific capacity of 3861 mAh g^{-1} and high negative potential of −3.05 V vs. NHE. However, lithium metal electrodes in contact with liquid electrolytes cause various problems, and the occurrence of dendrites formation during lithium deposition is particularly adverse, which leads to explosion hazards [1]. This phenomenon exists even with polymer electrolytes, although to a lesser extent than that with liquid electrolytes [2,3].

Lithium-air rechargeable batteries are an attractive energy storage system for electric vehicles (EV), because of their potential to provide acceptably high energy densities for EV applications [4]. They can yield a specific theoretical energy density as high as 11,140 Wh kg^{-1} (excluding oxygen), which is comparable to that calculated for gasoline. The typical lithium-air system consists of a lithium metal anode, a carbon electrode with a catalyst, and a non-aqueous electrolyte [5]. Nevertheless, it is difficult to exclude water from air in the air electrode using a conventional membrane filter, so that the lithium metal electrode may react with the water from the air. A water stable lithium electrode proposed by the current authors [6] has exhibited potential to prevent the reaction between water and lithium metal. The water stable lithium electrode consists of a lithium metal sheet as the active material, a polymer electrolyte buffer layer of poly(ethylene oxide) (PEO) with Li$(CF_3SO_2)_2N$ (LiTFSI), and a water stable NASICON-type lithium conducting solid electrolyte ($Li_{1+x+y}Ti_{2-x}Al_xP_{3-y}S_yO_{12}$). The polymer electrolyte hinders the direct contact of lithium metal and the solid electrolyte, because the solid electrolyte is unstable in contact with lithium. This three layer lithium electrode has been confirmed to have stability in water and exhibit reversible lithium dissolution and deposition with low polarization [7]. However, dendrite formation on the lithium electrode remains a problem when charging the cell.

Research addressing the mechanism of dendrite growth in Li/polymer electrolyte/Li has been extensively studied by Brissot et al. and Rosso et al. [2,3,8,9] by means of direct *in situ* observation and simultaneous evaluation of cell potential. They have reported that dendrite formation begins at a time t_0 and follows a power law as a function of the current density that is very close to Sand's law [10,11]. The relationship between the ionic concentration and the onset of dendritic growth was investigated by *in situ* and *ex situ* ionic concentration measurements in Li/polymer electrolyte/Li cells during cycling [12]. Brissot et al. [2] reported that dendrites are generated when the ionic concentration drops to zero at the

* Corresponding author. Tel.: +81 59 231 9420; fax: +81 59 231 9478.
E-mail address: imanishi@chem.mie-u.ac.jp (N. Imanishi).

0378-7753/$ – see front matter © 2011 Elsevier B.V. All rights reserved.
doi:10.1016/j.jpowsour.2011.04.001

negative electrode, and they also come to the conclusion that the apparent variation of the interface resistance was larger than that of the bulk resistance during polarization [9]. It is well known that a solid electrolyte interface (SEI) is created between lithium metal and a polymer electrolyte. The kinetics of dendrite formation is dependent on the properties of the SEI. Dendrite formation may be suppressed by using a polymer electrolyte that exhibits a low interface resistance with lithium metal. We have previously reported that the addition of nano-SiO_2 into PEO_{18}LiTFSI reduced the interface resistance of Li/polymer electrolyte/Li from 248 to 97.5 $\Omega\,cm^2$ at 60 °C and the short circuit time of 20 h at 0.5 mA cm^{-2} was prolonged to 42 h [13]. Furthermore, the short circuit time of a composite polymer electrolyte of PEO_{18}LiTFSI and *N*-methyl-*N*-propylpiperidinium bis(trifluoromethanesulfonyl)imide (PP13TFSI) [14] in Li/PEO_{18}LiTFSI-1.44PP13TFSI/Li cell was increased to 75 h at 0.5 mA cm^{-2}.

As a continuation of our previous research, a composite polymer electrolyte of PEO_{18}LiTFSI with a mixture of PP13TFSI and nano-SiO_2 was prepared and dendrite formation in the Li/PEO_{18}LiTFSI-SiO_2-PP13TFSI/Li cell was examined using direct *in situ* observation in the current density range from 0.1 to 1.0 mA cm^{-2}. We have observed that the dendrite formation in the Li/PEO_{18}LiTFSI-SiO_2-PP13TFSI/Li cell was improved further by the addition of nano-SiO_2 into PEO_{18}LiTFSI-PP13TFSI. In this study, the electrical conductivity of PEO_{18}LiTFSI-SiO_2-PP13TFSI and the interfacial resistance of Li/PEO_{18}LiTFSI-SiO_2-PP13TFSI/Li were examined and the relationship between lithium dendrite formation and the interfacial performance is discussed.

2. Experimental

PEO_{18}LiTFSI-SiO_2-PP13TFSI composite polymer electrolytes were prepared using a previously reported casting method [15]. LiTFSI (Fluka, USA) was completely dissolved in anhydrous acetonitrile (AN). SiO_2 (Kanto Chemicals, Japan, average particle size 50 nm) and PP13TFSI (Kanto Chemicals, Japan) were added into the solution and then PEO powder (Aldrich, USA, Mw = 6×10^5, Li/O = 1/18) was dissolved. The SiO_2 nano-powder was dried at 200 °C for 24 h under vacuum. The mole ratio of $Li^+/PP13^+$ was 1/1.44, which showed the best performance for suppression of the dendrite formation [14]. The content of nano-SiO_2 was 10 weight % (wt%) to PEO_{18}LiTFSI-1.44PP13TFSI. The mixture was stirred at room temperature for 24 h and the obtained homogeneous solution was then cast into a clean Teflon dish. The AN solvent was evaporated slowly at 40 °C in an Ar-filled glove box for 24 h and then dried at 100 °C for 24 h under vacuum. The obtained composite polymer electrolyte was a homogeneous film with an average thickness of 230 μm.

Sandwich cells of Au/PEO_{18}LiTFSI-SiO_2-PP13TFSI/Au with blocking electrodes were used for electrical conductivity measurements, and sandwich cells of Li/PEO_{18}LiTFSI-SiO_2-PP13TFSI/Li with non-blocking electrodes were used for measurement of the interface resistance and electrochemical properties. All cells were sealed in an Ar-filled dry glove box. The cell was sandwiched between two pieces of a plastic film with low water and gas permeability. The plastic film envelope was then evacuated and heat-sealed. Electrochemical impedance spectroscopy (EIS) measurements were conducted using a frequency response analyzer (Solartron 1260) with an electrochemical interface (Solartron 1287) in the frequency range from 1 MHz to 0.01 Hz. A nonlinear complex least squares fitting routine was used for data analysis.

An optical visualization cell was used for *in situ* examination of the formation and growth of lithium dendrites on the lithium/composite polymer electrolyte interface [13]. Two narrow lithium metal strips (0.4 mm wide and 0.02 mm thick) with copper

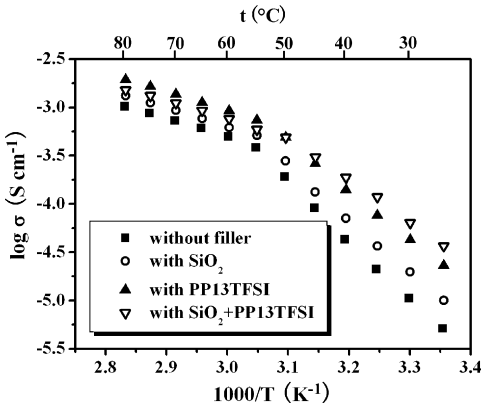

Fig. 1. Temperature dependence of the electrical conductivity for PEO_{18}LiTFSI, PEO_{18}LiTFSI-SiO_2, PEO_{18}LiTFSI-PP13TFSI and PEO_{18}LiTFSI-SiO_2-PP13TFSI.

film leads were placed end to end on the composite polymer electrolyte with a distance of ca. 1 mm between the two electrodes. The cells were sealed in the same manner as that for the sandwich cells. Dendrite growth was observed using a digital microscope (Keyence VHX-100).

3. Results and discussion

The electrochemical performance of lithium batteries with a metallic lithium anode depends on the properties of the solid electrolyte interface (SEI), and in particular, the composition and morphology of the SEI formed at the lithium surface. The SEI has a significant effect on lithium dendrite formation [16]. The SEI should protect further reaction of lithium metal and the electrolyte, and should have a high ionic conductivity at the operation temperature. The PEO based polymer electrolyte is stable with lithium metal, however, the interfacial resistance should be significantly reduced to obtain lower cell resistance [7]. The interfacial resistance of a typical polymer electrolyte of Li/PEO_{18}LiTFSI/Li is as high as 200 $\Omega\,cm^2$ at 60 °C and increases with the storage time. Moreover, dendrite formation during lithium deposition should be suppressed. In this study we have examined the effect of co-doping nano-SiO_2 and PP13TFSI into PEO_{18}LiTFSI on the interface resistance between lithium metal and the composite polymer electrolyte, and also on lithium dendrite formation.

Fig. 1 shows Arrhenius plots of the electrical conductivity for PEO_{18}LiTFSI-SiO_2-PP13TFSI, in addition to that for PEO_{18}LiTFSI, PEO_{18}LiTFSI-10 wt%-nano-SiO_2 and PEO_{18}LiTFSI-1.44PP13TFSI reported previously [14,15]. Conductivity enhancement at higher temperature by co-doping is not obvious, where the PEO melts, but at low temperature the enhancement by addition of both nano-SiO_2 and PP13TFSI is significant. The conductivity of PEO_{18}LiTFSI-SiO_2-PP13TFSI at 25 °C is 3.68×10^{-5} S cm^{-1}, which is higher than those for PEO_{18}LiTFSI-PP13TFSI (2.34×10^{-5} S cm^{-1}), PEO_{18}LiTFSI-SiO_2 (1.00×10^{-5} S cm^{-1}), and PEO_{18}LiTFSI (5.13×10^{-6} S cm^{-1}). The Arrhenius plots of all the electrolytes have a conductivity knee at 55 °C, which reflects the crystalline to liquid phase transition [17]. The activation energies for electrical conduction obtained from the Arrhenius plots are listed in Table 1. Addition of nano-SiO_2 and PP13TFSI to PEO_{18}LiTFSI results in a slight decrease of the activation energy in the low temperature region, while that in the high temperature region is almost constant. PEO_{18}LiTFSI with both nano-SiO_2 and PP13TFSI has the lowest activation energy, which suggests that the lithium cations are more mobile in the PEO chains [18].

The interface resistance dominates the cell resistance of the Li/PEO_{18}LiTFSI/Li cell. Previous studies [13,14] have shown that

Table 1
Electrical transport properties of $PEO_{18}LiTFSI$-X.

Sample $PEO_{18}LiTFSI$-X	Conductivity ($S\,cm^{-1}$)		Activation energy for conduction ($kJ\,mol^{-1}$)	
	25 °C	60 °C	Low temp. region	High temp. region
Without X	5.13×10^{-6}	4.96×10^{-4}	115.3	37.2
Nano-SiO_2	1.00×10^{-5}	6.20×10^{-4}	105.0	36.7
PP13TFSI	2.34×10^{-5}	9.20×10^{-4}	97.6	35.3
Nano-SiO_2 and PP13TFSI	3.68×10^{-5}	7.64×10^{-4}	82.9	35.1

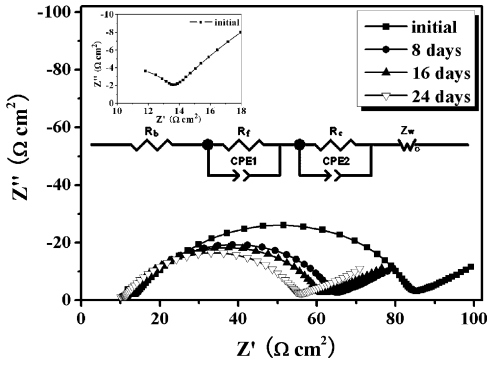

Fig. 2. Impedance spectra of Li/$PEO_{18}LiTFSI$-SiO_2-PP13TFSI/Li at 60 °C as a function of the storage time. The inset shows the impedance spectrum in a high frequency range.

the interfacial resistance between lithium metal and $PEO_{18}LiTFSI$ is approximately 250 Ω cm² at 60 °C and increases gradually with storage time, while the interface resistances of Li/$PEO_{18}LiTFSI$-SiO_2/Li and Li/$PEO_{18}LiTFSI$-PP13TFSI/Li are 108 Ω cm² and 98 Ω cm², respectively, and are stable with storage time. Fig. 2 shows typical impedance profiles for a Li/$PEO_{18}LiTFSI$-SiO_2-PP13TFSI/Li cell at 60 °C. These impedance spectra are very similar to those reported previously [13,14] and show a small semicircle in the high frequency range, as depicted in the inset of Fig. 2, and a large slightly depressed semicircle in the mid frequency range, followed by a straight line inclined at approximately 45°, which is typical of the diffusion phenomenon of ions. The small semicircle in the high frequency range could be assigned as the grain boundary resistance of the polymer electrolyte, because a similar small semicircle was observed in the same frequency range for a Au/$PEO_{18}LiTFSI$-SiO_2-PP13TFSI/Au cell. The high frequency intercept of the large semicircle with the real axis can be ascribed to the total resistance of the composite polymer, because the value is equal to that measured with the blocking electrode Au/$PEO_{18}LiTFSI$-SiO_2-PP13TFSI/Au cell at 60 °C. The diameter of the large semicircle is associated with the overall interface resistance (R_i), which consists of two parts; the resistance of the passivation film (R_f) formed on the lithium electrode surface by reaction with the polymer electrolyte and lithium metal (SEI), and the charge transfer resistance (R_c) of the $Li^+ + e^- = Li$ reactions [19]. The interface resistance of Li/$PEO_{18}LiTFSI$-SiO_2-PP13TFSI/Li cell decreased from 74 to 45 Ω cm² after storage at 60 °C for 24 days, which may be due to the reorganization of the passivation film during storage. Analysis of the impedance spectrum for the Li/$PEO_{18}LiTFSI$-nano-SiO_2-PP13TFSI/Li cell at the initial stage (after a few hours contact between lithium metal and the polymer electrolyte) yielded $R_f = 55.9\,\Omega\,cm^2$ and $R_c = 18.1\,\Omega\,cm^2$ at 60 °C, which are lower than those for Li/$PEO_{18}LiTFSI$-SiO_2/Li ($R_f = 77.2\,\Omega\,cm^2$ and $R_c = 29.8\,\Omega\,cm^2$) [13], and Li/$PEO_{18}LiTFSI$-PP13TFSI/Li ($R_f = 68.5\,\Omega\,cm^2$ and $R_c = 30.1\,\Omega\,cm^2$) [14].

Fig. 3 shows the inverse temperature dependence of the inverse specific surface passivation film resistance of R_f and the inverse specific charge transfer resistance of R_c for Li/$PEO_{18}LiTFSI$-SiO_2-PP13TFSI/Li. The Arrhenius plots of these interfacial resistances show no knee at the phase transition temperature observed in the conductivity measurement with the blocking Au/$PEO_{18}LiTFSI$-SiO_2-PP13TFSI/Au cell, which indicates that these interfacial resistances are not affected by the nature of the polymer electrolyte matrix, but by that of the passivation layer. The resistance of the SEI passivation layer at room temperature is significantly decreased by co-doping PP13TFSI and nano-SiO_2. The activation energy for the inverse resistance of the passivation layer decreased from 77.6 $kJ\,mol^{-1}$ for Li/$PEO_{18}LiTFSI$ to 63.5 $kJ\,mol^{-1}$ for $PEO_{18}LiTFSI$-SiO_2-PP13TFSI. The activation energy for the charge transfer between lithium metal and $PEO_{18}LiTFSI$-SiO_2-PP13TFSI of 79.2 $kJ\,mol^{-1}$ was not significantly different from that of Li/$PEO_{18}LiTFSI$/Li [14]. The activation energies for the inverse resistance of the passivation layer and the charge transfer between lithium metal and the electrolytes are summarized along with the interface resistances in Table 2, where the cell resistances after 24 days are also listed. The interface resistance of Li/$PEO_{18}LiTFSI$ after 24 days storage is considerably reduced

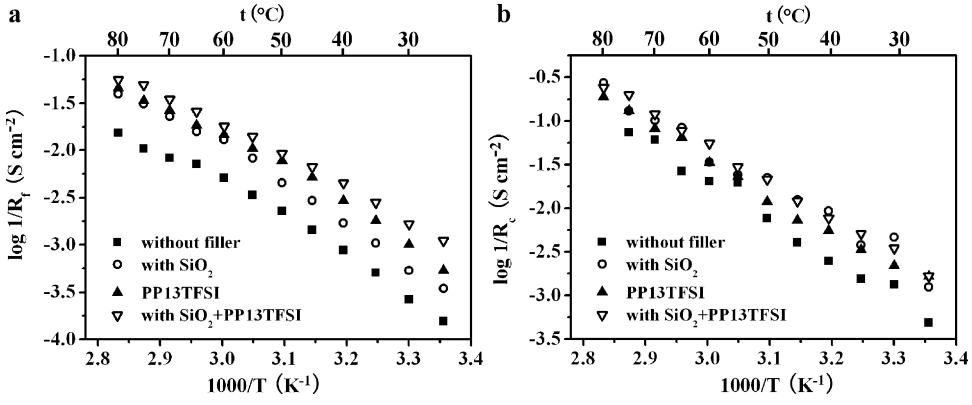

Fig. 3. Temperature dependence of the (a) inverse of the specific interface layer resistance R_f and (b) inverse of the specific charge transfer resistance R_c for Li/$PEO_{18}LiTFSI$/Li, Li/$PEO_{18}LiTFSI$-SiO_2/Li, Li/$PEO_{18}LiTFSI$-PP13TFSI/Li, and Li/$PEO_{18}LiTFSI$-SiO_2-PP13TFSI/Li.

Table 2
Cell resistance at 60 °C and activation energy for the inverse interface layer resistance (SEI) and inverse charge transfer resistance (CT) in Li/PEO_{18}LiTFSI-X/Li.

PEO_{18}LiTFSI-X	Interface resistance ($\Omega\,cm^2$)				Activation energy for the inverse interface resistance ($kJ\,mol^{-1}$)	Activation energy for the inverse charge transfer resistance ($kJ\,mol^{-1}$)
	SEI		CT			
	Initial	24 days	Initial	24 days		
Without X	199	398.7	49.4	53.0	77.6	79.1
Nano-SiO_2	77.2	67.9	29.8	30.8	77.8	77.4
PP13TFSI	68.5	74.2	30.1	22.1	68.7	79
Nano-SiO_2 and PP13TFSI	55.9	26.9	18.1	18.2	63.5	79.2

by co-doping of nano-SiO_2 and PP13TFSI in the polymer electrolyte.

The low lithium/polymer interface resistance leads to a low overpotential for lithium deposition and stripping on and from lithium metal, which is an important factor for the development of high power density lithium-air batteries [14,15]. Fig. 4 compares the deposition and stripping potentials after 2 h polarization vs. current density for Li/PEO_{18}LiTFSI/Li, Li/PEO_{18}LiTFSI-SiO_2/Li, Li/PEO_{18}LiTFSI-PP13TFSI/Li, and Li/PEO_{18}LiTFSI-SiO_2-PP13TFSI/Li at 60 °C. The polymer electrolyte without fillers and ionic liquid show high overpotentials, while the polymer electrolyte with nano-SiO_2, PP13TFSI, and a mixture of both exhibit lower overpotentials. The overpotential behaviors for Li/PEO_{18}LiTFSI-PP13TFSI/Li and Li/PEO_{18}LiTFSI-SiO_2-PP13TFSI/Li are almost the same. The low overpotentials may be due to the low cell resistance.

Besides the high electrical conductivity, stability with lithium metal, and low interface resistance between lithium metal and the electrolyte, the suppression of dendrite formation is another important requirement for an electrolyte with a lithium metal electrode for lithium-air batteries. The dendrite formation in Li/PEO_{18}LiTFSI-SiO_2-PP13TFSI/Li was examined using an optical visualization cell. Fig. 5 shows typical results at 0.5 mA cm^{-2} and at 60 °C. Dendrite formation was more suppressed by co-doping nano-SiO_2 and PP13TFSI formation and was observed after 46 h polarization of Li/PEO_{18}LiTFSI-SiO_2-PP13TFSI/Li, after which short-circuit was observed at 84 h. Table 3 summarizes the dendrite formation onset time and short-circuit time for the polymer electrolyte with various dopants. The dendrite formation onset time and short-circuit time were prolonged by the addition of both SiO_2 and PP13TFSI. The specific capacities of a lithium electrode with a 10 μm thick copper substrate for the PEO_{18}LiTFSI-SiO_2-PP13TFSI composite electrolyte were calculated to be 1966 mAh g^{-1} at 1.0 mA cm^{-2} and 2154 mAh g^{-1} at 0.5 mA cm^{-2}, which is a further improvement over that previously reported [13,14].

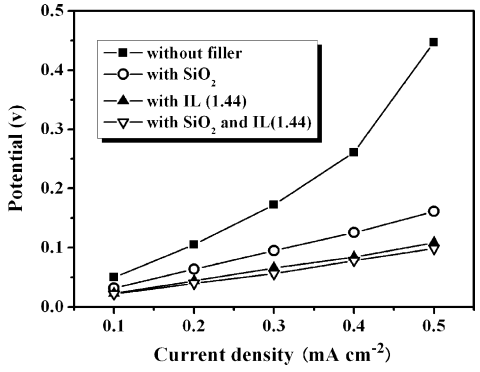

Fig. 4. Current density vs. polarization potential curves for Li/PEO_{18}LiTFSI/Li, Li/PEO_{18}LiTFSI-SiO_2/Li, Li/PEO_{18}LiTFSI-PP13TFSI/Li, and Li/PEO_{18}LiTFSI-SiO_2-PP13TFSI/Li at 60 °C.

Rosso et al. [8] reported the relation between the onset time (t_0) of dendrite formation and the polarization current (J) for Li/PEO-LiTFSI/Li at 90 °C. The dendrite formation onset time followed a power law as a function of the current, very close to Sand's law [11] in the current range of 0.03–0.3 mA cm^{-2},

$$t_0 = \pi D\left(\frac{eC_0}{2J}\right)^2\left(\frac{\mu_a+\mu_c}{\mu_a}\right)^2, \quad (1)$$

where C_0 is the initial concentration, D is the ambipolar diffusion constant, and μ_a and μ_c are the anionic and cationic mobilities, respectively. The $\log t_0$ vs. $\log J$ curve for Li/PEO_{18}LiTFSI-SiO_2-PP13TFSI/Li at 60 °C is shown in Fig. 6. The curve shows good linearity in the range of 0.1–1.0 mA cm^{-2} with a slope of −1.34. In previous work [13,14] the line slopes were −1.25 and −1.30 for the nano-SiO_2- and PP13TFSI-doped systems. The similarity of the three samples indicates that the mechanism for improvement is basically the same. According to Eq. (1), the dendrite onset time is dependent on the diffusion constant of lithium ions in the electrolyte, which is related to the inverse of the passivation resistance from the Nernst and Einstein equation. The linear relationship between $1/R_f$ and t_0 is shown in Fig. 7, where t_0 was collected at 0.5 mA cm^{-2}. This result suggests that the dendrite formation on lithium metal is associated with the resistance of the SEI between lithium and the polymer electrolyte, as expected from Eq. (1).

Fig. 8 shows the cycling performance of the lithium deposition and stripping process in Li/PEO_{18}LiTFSI-SiO_2-PP13TFSI/Li at 60 °C, where a constant current of 0.3 mA cm^{-2} was passed for 30 h during each process. No significant change in cell voltage was observed during the cycles, and microscopic observations of the cell indicated no dendrite formation after the cycling test as shown in Fig. 9. The capacity of 9 mAh cm^{-2} (0.3 mA cm^{-2} × 30 h) corresponds to the specific capacity of 980 mAh g^{-1} for the anode with a 10 μm

Table 3
Dendrite formation onset time (t_0) and short-circuit time (t_s) at different polarization current densities for Li/PEO_{18}LiTFSI-X/Li at 60 °C.

PEO_{18}LiTFSI-X	Current density (mA cm^{-2})	t_0 (h)	t_s (h)	References
Without X	0.1	125	225	[13]
	0.25	60	76	
	0.5	15	20	
	1.0	10	15	
Nano-SiO_2	0.1	205	355	[13]
	0.25	70	90	
	0.5	25	40	
	1.0	10–15	15	
PP13TFSI	0.1	434	594	[14]
	0.25	105	135	
	0.5	35	75	
	1.0	17	35	
Nano-SiO_2 and PP13TFSI	0.1	460	672	This work
	0.25	110	168	
	0.5	46	84	
	1.0	21	37	

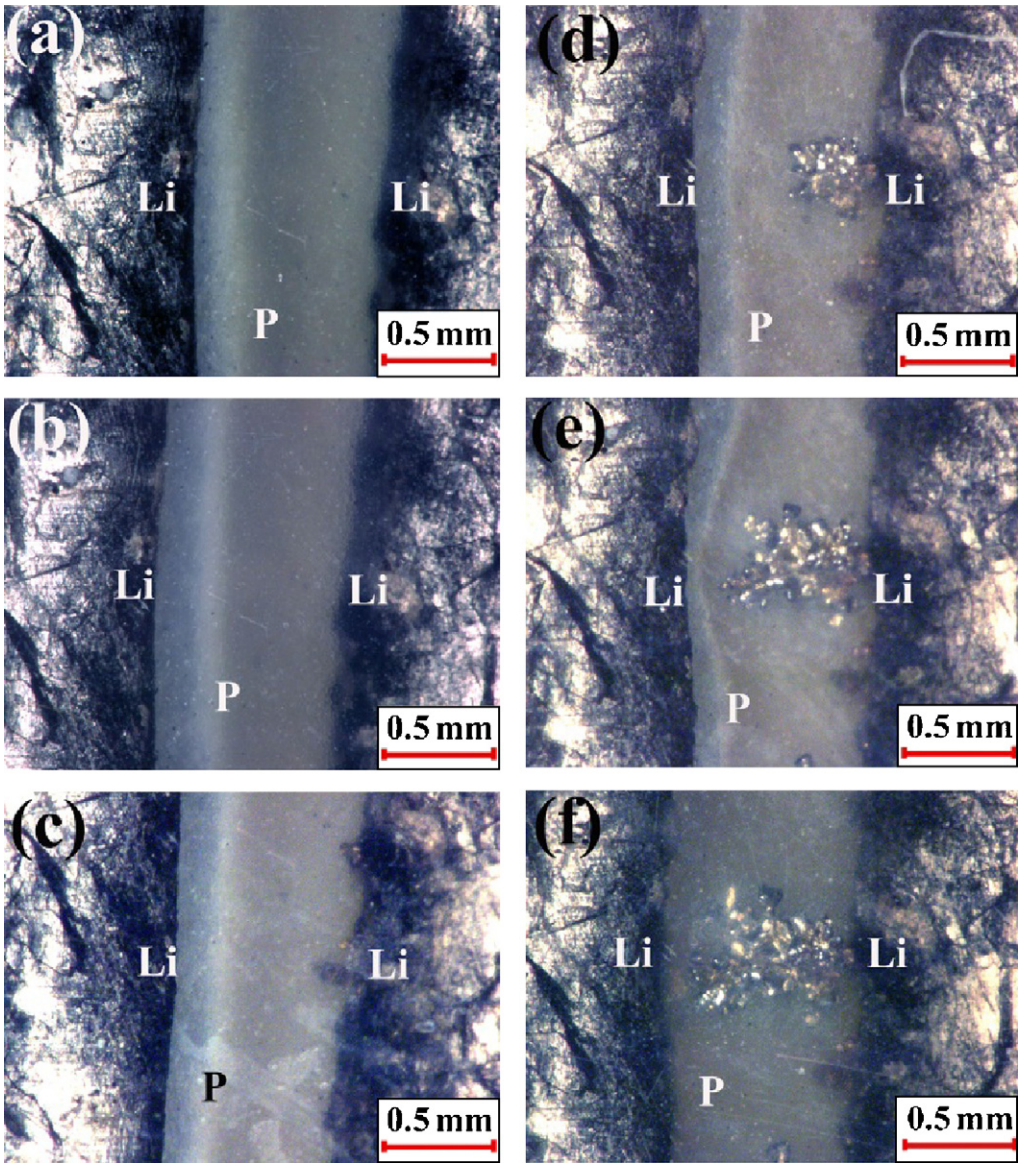

Fig. 5. Visualization of dendrite growth in the Li/PEO_{18}LiTFSI-SiO_2-PP13TFSI/Li cell at 60 °C and 0.5 mA cm^{-2} at t = (a) 0, (b) 40, (c) 46, (d) 60, (e) 76, and (f) 84 h.

thick copper substrate. The capacity is two times higher than that of a carbon anode.

Compared to PEO_{18}LiTFSI-SiO_2 and PEO_{18}LiTFSI-PP13TFSI, the PEO_{18}LiTFSI electrolyte co-doped with nano-SiO_2 and PP13TFSI exhibits better performance for suppression of lithium dendrite formation, which is explained by the low resistance of the interface layer between lithium and the polymer electrolyte. This may be due to a synergistic effect of nano-SiO_2 and PP13TFSI. The

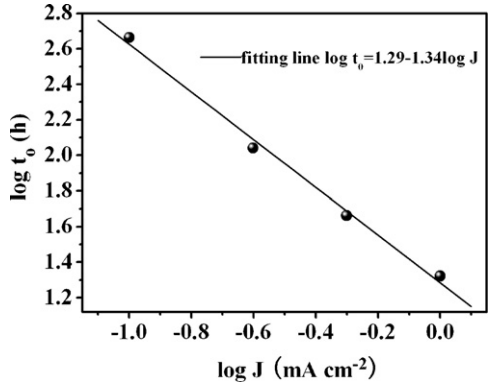

Fig. 6. Log current density (J) vs. log dendrite formation onset time (t_0) for Li/PEO_{18}LiTFSI-SiO_2-PP13TFSI/Li at 60 °C.

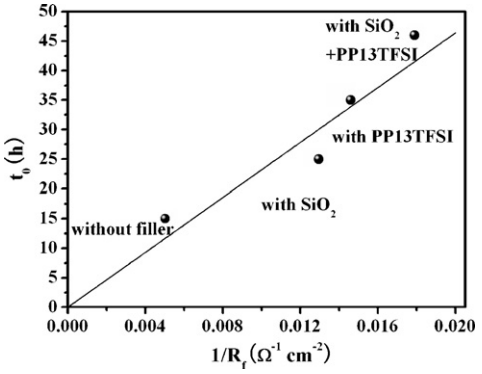

Fig. 7. Relationship between the dendrite formation onset time (t_0) and the inverse of the specific interface layer resistance between Li and PEO-based electrolytes at 60 °C.

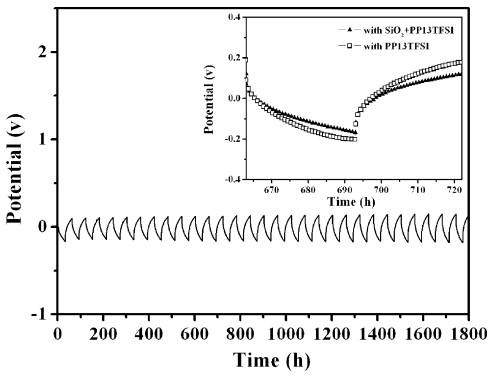

Fig. 8. Cycling performance for the Li/PEO_{18}LiTFSI-SiO_2-PP13TFSI/Li cell at 60 °C and 0.3 mA cm^{-2} for 30 h polarization. The inset shows a comparison of the 11th cycle for Li/PEO_{18}LiTFSI-SiO_2-PP13TFSI/Li and Li/PEO_{18}LiTFSI-PP13TFSI/Li.

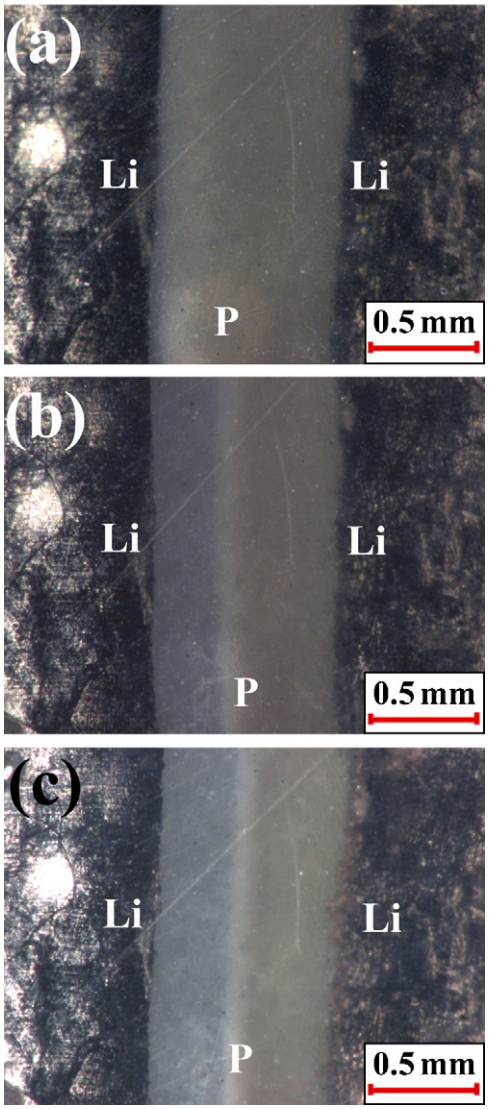

Fig. 9. Visualization of dendrite growth in the Li/PEO_{18}LiTFSI-SiO_2-PP13TFSI/Li cell at 60 °C and 0.3 mA cm^{-2} for 30 h polarization (a) before cycle, (b) after 15 cycles and (c) after 30 cycles.

conductivity enhancement of PEO_{18}LiTFSI by addition of SiO_2 could be explained by Lewis acid–base type surface interaction of ionic species with O/OH groups on the filler surface [20], and the addition of PP13TFSI plays a positive role in the formation of the passivation film, which leads to lower resistance of the interface film [21]. The physical and chemical properties of the interface layer should be studied in more detail and this research is ongoing.

4. Conclusion

The electrical conductivity of 5.13×10^{-6} S cm^{-1} for PEO_{18}LiTFSI at 25 °C is enhanced to 3.68×10^{-5} S cm^{-1} at 25 °C by doping with a mixture of nano-SiO_2 and PP13TFSI. The Li/PEO_{18}LiTFSI-SiO_2-PP13TFSI/Li cell exhibited a stable and low interface resistance of 74 Ω cm^2 at 60 °C.

Lithium dendrite growth was observed using an optical visualization cell. The dendrite formation on lithium metal by lithium deposition was effectively suppressed by the addition of a mixture of nano-SiO_2 and PP13TFSI into PEO_{18}LiTFSI. The onset time of dendrite formation of 15 h for Li/PEO_{18}LiTFSI/Li at 0.5 mA cm^{-2} and 60 °C was improved to 46 h under the same conditions by addition of the nano-SiO_2 and PP13TFSI mixture into PEO_{18}LiTFSI. The specific weight capacity of a lithium metal anode with a 10 μm thick copper current collector was calculated to be 1458 mAh g^{-1} at 1.0 mA cm^{-2} and 1543 mAh g^{-1} at 0.5 mA cm^{-2}. The composite solid polymer electrolyte is quite attractive as a buffer layer between a lithium anode and water stable lithium conducting NASICON-type solid electrolyte for lithium-air batteries and also as an electrolyte for all solid state batteries with lithium metal anodes.

Acknowledgment

This work was supported by the New Energy and Industrial Technology Development Organization (NEDO) of Japan under the "Development of High Performance Battery System for Next Generation Vehicles" project.

References

[1] J.M. Tarascon, M. Armand, Nature 414 (2001) 359.
[2] C. Brissot, M. Rosso, J.N. Chazalviel, S. Lascaud, J. Power Sources 81 (1999) 925.
[3] C. Brissot, M. Rosso, J.N. Chazalviel, P. Baudry, S. Lascaud, Electrochim. Acta 43 (1998) 1569.
[4] M. Armand, J.M. Tarascon, Nature 451 (2008) 652.
[5] T. Ogasawara, A. Debart, M. Holzapfel, P. Novak, P.G. Bruce, J. Am. Chem. Soc. 128 (2006) 1390.
[6] T. Zhang, N. Imanishi, H. Hasegawa, A. Hirano, J. Xie, Y. Takeda, O. Yamamoto, N. Sammes, J. Electrochem. Soc. 155 (2008) A905.
[7] T. Zhang, N. Imanishi, S. Hasegawa, A. Hirano, J. Xie, Y. Takeda, O. Yamamoto, N. Sammes, Electrochem. Solid-State Lett. 12 (2009) A132.
[8] M. Rosso, T. Gobron, C. Brissot, J.N. Chazalviel, S. Lascaud, J. Power Sources 97–98 (2001) 804.
[9] M. Rosso, C. Brissot, A. Teyssot, M. Dolle, L. Sannier, J.M. Tarascon, R. Bouchetc, S. Lascaud, Electrochim. Acta 51 (2006) 5334.
[10] M. Rosso, E. Chassaing, V. Fleury, J.N. Chazalviel, J. Electroanal. Chem. 559 (2003) 165.
[11] H.J.S. Sand, Philos. Mag. 1 (1901) 45.
[12] C. Brissot, M. Rosso, J.N. Chazalviel, S. Lascaud, J. Power Sources 94 (2001) 212.
[13] S. Liu, N. Imanishi, T. Zhang, A. Hirano, Y. Takeda, O. Yamamoto, J. Yang, J. Power Sources 195 (2010) 6847.
[14] S. Liu, N. Imanishi, T. Zhang, A. Hirano, Y. Takeda, O. Yamamoto, J. Yang, J. Electrochem. Soc. 157 (2010) A1092.
[15] Y. Liu, Y. Takeda, T. Matsumura, J. Yang, N. Imanishi, A. Hirano, O. Yamamoto, J. Electrochem. Soc. 153 (2006) A437.
[16] A. Teyssot, M. Rosso, R. Bouchet, S. Lascaud, Solid State Ionics 177 (2006) 141.
[17] Y.G. Andreev, P.G. Bruce, Electrochim. Acta 45 (2000) 1417.
[18] W.H. Meyer, Adv. Mater. 10 (1998) 439.
[19] G.B. Appetecchi, F. Croce, G. Dautzenberg, M. Mastragostino, F. Ronci, B. Scrosati, F. Soavi, A. Zanelli, F. Alessandrini, P.P. Prosini, J. Electrochem. Soc. 145 (1998) 4126.
[20] M. Dissanayake, P. Jayathilaka, R.S.P. Bokalawala, I. Albinsson, B.E. Mellander, J. Power Sources 119 (2003) 409.
[21] Y.H. Kim, G. Cheruvally, J.W. Choi, J.H. Ahn, K.W. Kim, H.J. Ahn, D.S. Choi, C.E. Song, Macromol. Symp. 249 (2007) 183.